



AVSAP

Autonomous Voltage Spike Analysis Program

Technical Division, Magnet Systems Department

Author: Said Rahimzadeh-Kalaleh

Supervisor: Michael Tartaglia, Ph.D.

August 3, 2007

Abstract

With the upcoming inauguration of the Large Hadron Collider (LHC) at CERN, a limit in the maximum magnetic field achievable through NbTi superconductors will be reached based on the properties of the material. Fermilab has been developing a new generation of superconducting accelerator magnets based on Nb₃Sn. The performance of these magnets has been found to be below the expected in terms of its critical current density due to thermo-magnetic instabilities present in the superconductor. In order to develop better magnets for future machines, it is essential to fully understand these instabilities. Several analytical studies have been done, but a quantitative analysis on the voltage spikes representing these instabilities has been limited by the high amount of transients that need to be processed. In this paper, I present the functionality and features of the first software designed at Fermilab to perform an analytical and quantitative study on voltage spikes in superconducting Nb₃Sn strands, cables, and magnets.

Contents

1. Introduction	6
1.1. Introduction to Fermilab	6
1.2. Background on Superconductivity	6
1.3. Scope of My Work at Fermilab	7
2. Voltage Spike Studies on Nb₃Sn	7
2.1. Previous Work	7
2.2. Present Voltage Spike Detection System	8
2.3. The need for a new software	10
3. AVSAP's Functionality	10
3.1. Data Acquisition	10
3.2. Data Processing	11
3.3. AVSAP's Adjustable Parameters	12
3.4. Graphical User Interface	13
3.5. Single File Processing Options	14
3.6. Multiple File Processing Options	20
4. Results	24
5. A Branch Project: Filtering Analysis for Half Coil Voltage Signals in SC Magnets and Implications for Future Studies	26
5.1. Previous Filtering Analysis	26
5.2. A Series of Low-Pass Filters	27
5.3. Choosing an Adequate Filter	33
6. Conclusions	43
7. Acknowledgments	43
A. AVSAP GUI	45

List of Figures

1.	Critical Surface for Nb ₃ Sn	8
2.	VSDS Circuit Block Diagram	9
3.	Sample Figure for Current Output	15
4.	Sample Figure for Voltage Output	15
5.	Sample Figure for Filtered Voltage Signal Output	16
6.	Sample Figure for Spectrum Analyzer Output	16
7.	Sample Figure for Filtered Spectrum Analyzer Output	18
8.	Sample Figure for FFT Output	18
9.	Sample Figure for Filtered FFT Output	19
10.	Sample Figure for Numbered Peak Magnitude Output	19
11.	Sample Figure for View Spikes Output	20
12.	Export to Excel Prompt and Output	20
13.	Sample Figure for I-V Profile Output	22
14.	Sample Figure for 3D I-V Profile Output	23
15.	Sample Figure for Voltage Histogram Output	23
16.	Sample Figure for Current Histogram Output	25
17.	AVSAP v.s. Human Spike Detection	25
18.	Current signal for the file under consideration	28
19.	Voltage Signal Prior to Filtering.	28
20.	Spectral Components of the Voltage Signal to Which the Filter is Applied.	29
21.	Accepted Spectral Components of Voltage Signal After First Filter	29
22.	Reconstructed Voltage Signal After First Filter	30
23.	Accepted Spectral Components of Voltage Signal After Second Filter	30
24.	Reconstructed Voltage Signal After Second Filter	31
25.	Effects of Different Low-Pass Filters on Noise	32
26.	SRR Distribution After a 30 kHz Low-Pass Filter	34
27.	SRR Distribution After a 25 kHz Low-Pass Filter	35
28.	SRR Distribution After a 20 kHz Low-Pass Filter	36
29.	SRR Distribution After a 15 kHz Low-Pass Filter	37
30.	Distribution of Spikes with SRRs Above 0.1 After a 30 kHz Low-Pass Filter	39
31.	Distribution of Spikes with SRRs Above 0.1 After a 25 kHz Low-Pass Filter	40
32.	Distribution of Spikes with SRRs Above 0.1 After a 20 kHz Low-Pass Filter	41

33. Distribution of Spikes with SRRs Above 0.1 After a 15 kHz Low-Pass Filter 42

1. Introduction

1.1. Introduction to Fermilab

Supported by the U.S. Department of Energy, Fermi National Accelerator Laboratory (Fermilab) advances the understanding of the fundamental nature of matter and energy by providing leadership and resources for qualified researchers to conduct basic research at the frontiers of high energy physics and related disciplines. Fermilab is composed of 10 Division/Sections, one of which is the Technical Division. Under the Technical Division lies the Magnet Systems Department, which provides support for the Fermilab Accelerator complex by repairing or refurbishing existing accelerator components and designing, fabricating and providing testing oversight of new devices for improvements to the accelerator complex. As an intern at Fermilab, I worked under the Magnet Systems Department, with the Measurements and Analysis Group. This group is involved in magnetic measurements of all types of magnets, and quench performance & conductor characterization of superconducting magnets.

1.2. Background on Superconductivity

Just three years after succeeding in liquifying helium, K. Onnes along with a graduate student at the Leiden Laboratory discovered that at a temperature T_c near 4 K the electrical resistance of Mercury completely vanished. It was Onnes who realized that the sample being studied had undergone a transformation into a new state, which he called 'superconductivity'. The temperature of the transition from the normal to the SC state, T_c , was called the critical temperature. Although the SC state was shortly achieved for several other metals such as tin, lead, indium, aluminum, and niobium, some of the best known normal conductors such as gold and copper have not yet shown to be SC at the lowest accessible temperatures.

In the years after the discovery of superconductivity, it was realized that the SC state may not only be destroyed by exceeding the critical temperature T_c , but also by exceeding a critical external magnetic field B_c and a critical current density J_c . In general, these three parameters depend on each other.

$$T_c = (B_c, J_c), \quad B_c = (T_c, J_c), \quad J_c = (T_c, B_c) \quad (1)$$

The critical surface of Nb₃Sn, the superconductor of choice for the new generation of accelerator magnets, is shown in Figure 1. This surface represents the boundary between

the SC and the normal state. Basically, for any point provided by the critical parameters of the superconductor lying inside the critical surface, the material is in the SC state. The transition of a superconductor back to the normal state, that is, when it goes outside the critical surface, is called a quench.

The literature on superconductivity is vast, so fundamental aspects such as the Meissner-Ochsenfeld effect and London Penetration Depth, or the distinction between type I and type II superconductors are omitted from this paper for brevity. However, the interested reader may see for example, [1], for a comprehensive study on superconductivity or, [2] and [3], for a more specific discussion on SC magnets. Nevertheless, I state here that Nb_3Sn is a type II superconductor, which is of utmost importance to the present discussion. Type II superconductors allow flux jumping while remaining in the SC state, which is the property responsible for the voltage spikes here discussed. For a rigorous mathematical representation on flux creep and flux jumping, see for example [4].

1.3. Scope of My Work at Fermilab

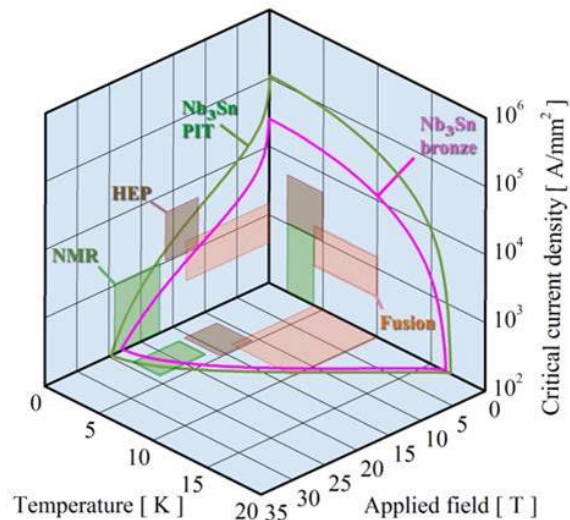
During my internship at Fermilab, I worked on several projects involving both SC and normal accelerator magnets. My work on conventional magnets involved a reliability study on the magnets of Fermilab's Main Injector (FMI) in light of its implications to the International Linear Collider (ILC). An abstract for the publication of this work, with Michael Tartaglia (my supervisor) as the main author, has been accepted by the Magnet Technology 20th Conference.

The present paper, however, focuses on my main project at Fermilab, which was the creation of a custom designed software to perform an analytical and quantitative study on voltage spikes in SC Nb_3Sn strands, cables, and magnets. This software, titled Autonomous Voltage Spike Analysis Program (AVSAP) will remain at Fermilab's Magnet Systems department for further use. The drivers for the development of AVSAP and the program's functionality and features are presented next.

2. Voltage Spike Studies on Nb_3Sn

2.1. Previous Work

Throughout the R&D process of Nb_3Sn SC magnets at Fermilab, voltage spikes have been extensively observed in signals from magnet half-coils, Rutherford type cables, and single

Figure 1: Critical Surface for Nb₃Sn

strands. These voltage spikes are known to arise either from flux jumps or mechanical motion of the superconductor [5]. Some classification of these voltage spikes has been done [6], and a model to calculate magnetic instabilities in SC wires with transport current has been developed [7]. As described in [8], the most noticeable features of the spikes analyzed include propagation and coupling. Voltage spike signals have been correlated with quench antenna signals [9], indicating these are magnet phenomena. Of great importance is the fact that these instabilities in SC magnets can result in premature quenching. Therefore, fully understanding the nature of these instabilities as well as its effects is essential to improve the performance of the new generation of SC accelerator magnets.

2.2. Present Voltage Spike Detection System

By fixing the critical parameters B_c and T_c , the critical current density, J_c , of a superconductor can be studied. The basic procedure in this studying consists of energizing the superconductor by "ramping" the current gradually until the magnet quenches. It is during this ramping that the voltage spikes of interest are observed. To detect these transients, the Magnet Systems Department at Fermilab relies on a system called *Voltage Spike Detection System* (VSDS), which was designed at Fermilab and consists of both hardware and software. The VSDS circuit block diagram is shown in Figure 2.

After the analog data has been acquired, it is digitized by the National Instruments (NI) PXI multifunction DAQ. The NI PXI has 4 channels of simultaneous Analog to Digital

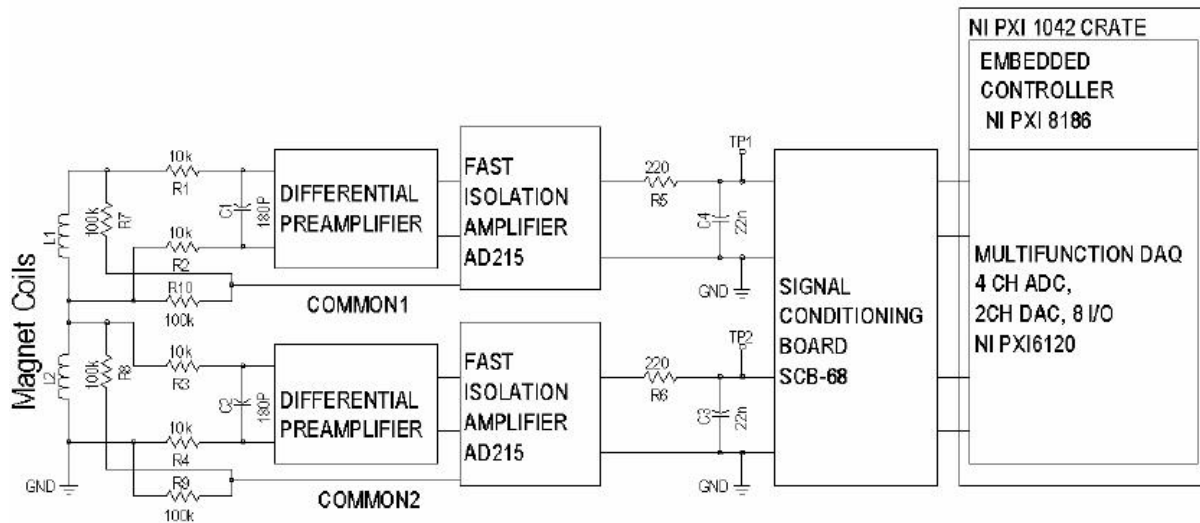


Figure 2: VSDS Circuit Block Diagram

Converters (ADC) with 16-bit resolution. After going through the ADCs, the digital data representing the acquired voltage signals are essentially tested by an algorithm with an "if" statement. The condition is,

$$if (|V_1 - V_2| \geq T) \longrightarrow CF \quad (2)$$

where V_i is the voltage of the i^{th} half-coil, T is the voltage threshold value set by the user at the time of ramping the magnet, and CF is the creation of a file with the event of interest.

Essentially, the VSDS software creates a file containing half a second of data every time the system detects a difference between the two "half-coil" voltages exceeding a user-defined (noise limited) threshold. The VSDS software was developed in Labview, but the files created may be converted into Matlab (.mat) files. Every half a second of data contains 50,000 data points for each one of the three signals present, V_1 , V_2 , and I . The sampling rate, which is 100,000 data points/sec is responsible for the amount of data points present for each signal in the files. For a more complete description of the VSDS and probing setup, the interested reader may see for example [11] or [8].

2.3. The need for a new software

Although the VSIDS is effective in creating data files containing the voltage and current signals of the superconductor whenever the voltage exceeds a certain threshold value, it has no analytical tools for post-processing these files. Specifically, once the data file is created, there is no automatic way to scan the files and detect the peak voltage of every spike, its width, and the value for the current at the time of the spike. All of these desired characteristics of a spike pose what is perhaps the most essential question to my work; that is, What constitutes a spike ?

In order to develop a software capable of providing the desired information described above, an algorithm relying on a mathematical formulation to detect the spikes is needed. The program needs to be flexible, allowing the user to easily adjust the parameters defining what constitutes a spike. Prior to my arrival, this kind of software had not been done for this application. Voltage Spikes had been studied by manually scanning file by file (one at a time) in search for any spike. The user, which was commonly a student, searched for these spikes in a graphical interface which allows a single event (half a second) to be displayed. Through this software, which was created by a scientist from Fermilab , the student determined what the peak voltage and the instantaneous current was at the time of any spike present in the signal. This slow, laborious process was repeated several hundred times, in order to create valuable statistics needed to characterize trends for each type of superconductor tested.

3. AVSAP's Functionality

3.1. Data Acquisition

AVSAP is a stand alone executable developed on MATLAB, which means that it may run on any machine regardless of MATLAB's presence. Once the user selects the file(s) to be processed, AVSAP reads voltage and current signals directly from these files, which are automatically generated by the VSIDS while the current in a magnet is ramped until it quenches. The files include half a second of data for the signals under consideration, as well as the essential parameters for the analysis of the files such as the amplifier's gain, voltage threshold value for triggering the DAQ (Data Acquisition) system, and the sampling rate. All files created by the VSIDS are arranged as structures containing the actual current and

voltage data points in arrays of 'double' precision elements, and the other parameters as 'char' type elements.

3.2. Data Processing

After reading the signals and obtaining the parameters affecting them, AVSAP then proceeds to detect the peaks in the voltage signal of the file(s) processed. Several methods were considered, but only two different ones were employed successfully to detect the spikes. First, the spikes were detected by means of wavelet transforms. The author was led to use wavelets due to the high amount of noise present in the signals, which makes it ideal for a multi-resolution analysis. An algorithm based on a continuous wavelet transform was found to be highly precise in detecting the spikes. However, to scan an entire ramp (100 - 150 files), the algorithm takes between 2 and 3 hours to perform the analysis.

Seeking to diminish the processing time, a new algorithm (which is the one currently used by AVSAP) was developed. This second algorithm relies on the application of 15 kHz low-pass filter to the signal. The filtering is done by first switching the signal to the frequency domain by means of the FFT (Fast Fourier Transform). Once in the frequency domain, all spectral components above 15 kHz are set equal to 0, which results in a low pass filter. Next, the signal is reconstructed with the remaining frequencies only (0-15 kHz) by means of the IFFT (Inverse Fast Fourier Transform). Although the filtered signal loses a bit of amplitude, the SNR (signal to noise ratio) is improved drastically (*more on this in section 5*). The new SNR was so good that the well known method of detecting peaks by zero crossings of the first derivative was able to be implemented. To prevent detection of false spikes, this second algorithm requires a peak to comply with other parameters (*see section 3.3*) such as amplitude threshold and width threshold in order to be declared as a spike.

Another added feature on the data processing of the new algorithm is a user friendly filter design platform. By pressing on the filter adjust button (*see section 3.3*), the user may change the default 15 kHz low-pass filter applied to the data before looking for the spikes. Once the spikes are localized in time, the algorithm goes back to the original signal and looks for the peak voltage in that region (± 2 msec). This way, the user may be assured that the peak voltage being registered is that of the original signal, and not that of the filtered signal. This process of returning to the original signal is motivated by the observation that as a greater part of the upper end of the spectrum is filtered, the signal loses more amplitude. To arrive to this conclusion, the author performed a detailed analysis on the effect different types of filters have on the signal (*see section 5*).

Although the second algorithm is less elegant than the one using wavelets, it takes less than a minute to obtain all the spikes of an entire ramp with good accuracy and precision, compared to 2-3 hours. Therefore, AVSAP uses the second algorithm. Depending on the number of files being processed, AVSAP allows the user to analyze the signals and the spikes found through different tools. The program by itself is capable of generating a variety of plots and statistics for single and multiple file processing. Also, the user may export the data from any type of processing to MS Excel as a matrix containing the file number, spike number (within the file), current at the time of the spike, the spike's peak voltage, and approximate width (in ms) of each spike. The complete source code for AVSAP is several thousand lines of code in length.

3.3. AVSAP's Adjustable Parameters

The spike detection algorithm relies on several parameters to discriminate 'real' from 'false' spikes. These parameters may be adjusted by the user by pressing on the buttons with the following names.

↔ Adjust Amplitude Threshold

By pressing this button, the user has the option to adjust the amplitude threshold for a spike. This threshold represents the lowest value (in mV) a peak needs to have in order to be called a spike by the spike detection algorithm. The default value is 25 mV, which is slightly above the highest values of noise observed (after the filtering) in the particular magnets TQS02a and TQC01b at the time of creating AVSAP. This value will remain as such unless the user changes it.

↔ Adjust Width Threshold

Pressing this button allows the user to change the default value provided to the searching algorithm as the expected number of data points that will be present in a typical spike.

↔ Absolute Value

This button allows the user to select an output format for the values of the spike's peak voltages. If the user selects "Absolute Value," the absolute value of the voltages will be taken. However, if "Positive and Negative" is selected, both sign and magnitude will be

displayed. This feature was added based on the fact that in general, the user is only interested in detecting the magnitudes of the voltage spikes, and is not interested in determining which coil (in the case of half-coils) was at a higher electric potential.

↔ Filter Adjust

When the user presses this button, the 15 kHz filter may be changed through a prompt that asks for the new limits of a band-pass filter. The minimum allowed frequency is zero (resulting in a low-pass filter), while the maximum allowed frequency is 50 kHz (based on the sampling rate).

↔ Show Parameters Used

At any instant, the user may choose to display a window showing the parameters being used by AVSAP for the automated analysis. This window includes the information regarding all the parameters described above plus the VSDS voltage threshold value, T , set by the scientist ramping the magnet. From the parameters arising from the hardware part of the VSDS, only T was chosen to be displayed because this is the only dynamic parameter. While T may be changed at any instant by the person ramping the magnet depending on the amount of noise observed during the ramp, the other parameters such as the amplifiers' gain or the sampling rate never change during a ramp.

3.4. Graphical User Interface

All features of AVSAP are provided to the user through a user friendly Graphical User Interface (GUI), which was created by Conor Donnelly, the author's colleague at the SIST program from the University of Pennsylvania. When AVSAP is executed, the user has the option to analyze many files or one file. Depending on the choice of the user, he/she will be led to one of two different platforms which include somewhat different buttons and functionality. The main motivation to have different platforms for single file processing and many files processing is the type of post-processing analysis that may be performed on the files of interest. Namely, when processing many files the user may be more interested in the statistics regarding the spikes detected, which may have no meaning for a single file. On the other hand, when processing a single file the user may be interested in features such as a detailed spectrum analysis, which may become tedious and unnecessary when processing multiple files.

The GUI has push-buttons and toggle-buttons. A push-button is a button that, when pressed, will execute an action immediately. A toggle-button is a button that allows the user to select the feature to be displayed prior to the processing. The user may see that a toggle button has been pressed when an asterisk is appended to the button.

3.5. Single File Processing Options

If the user selects to process a single file, he/she may start the processing by clicking on the button "Choose File and Execute". This will open a Java interface allowing the user to select a single file to be processed. The program then proceeds to find all the spikes within the selected file and saves all figures on a temporary directory for later calling. After the file has been processed (typically < 3 sec.) the user may view a plot of any of the analytical tools provided by AVSAP by pressing on the corresponding buttons. Alternatively, any plot can be displayed in a new window by pressing "Show Current Figure in New Window".

The features available in AVSAP when a single file is processed are presented next. Sample outputs of pressing each button in the single file processing mode are shown in Figures 3-12. All figures in this section correspond to the same file.

▷ Current (Figure 3)

This button displays the current signal (in Amps) versus time.

▷ Voltage (Figure 4)

This button displays the raw, unfiltered voltage difference signal (in mV) versus time.

▷ Filtered Voltage Signal (Figure 5)

This button displays the filtered voltage difference signal versus time (according to the parameters set by the user).

▷ Spectrum Analyzer (Figure 6)

This button displays the original voltage signal in the frequency domain, with power density on the y-axis. This feature simulates the effect a spectrum analyzer would have on the signal.

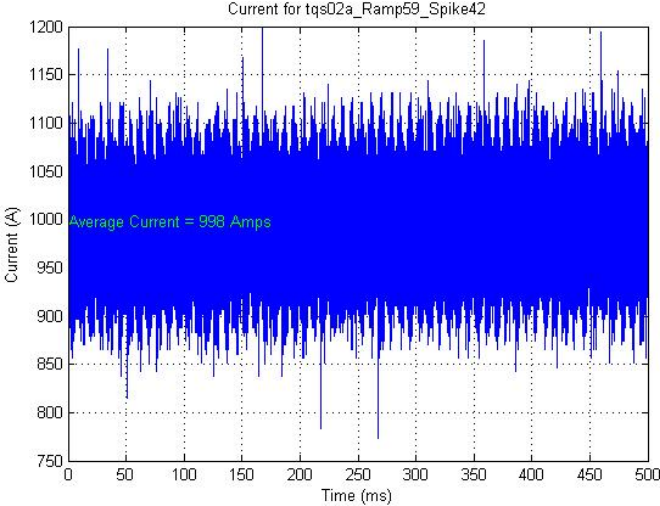


Figure 3: Sample Figure for Current Output

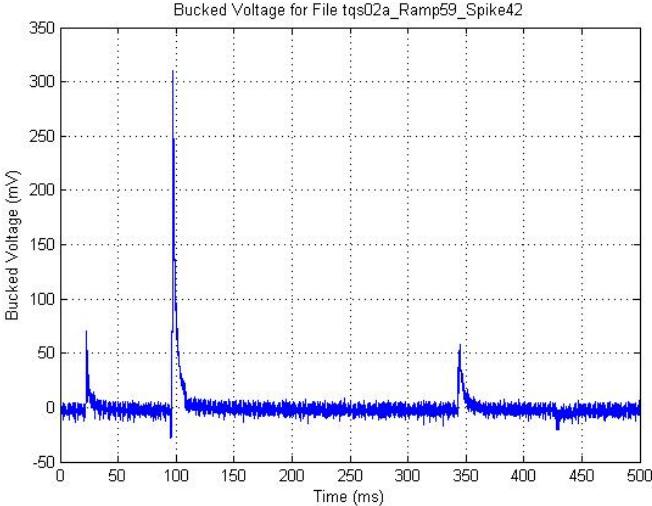


Figure 4: Sample Figure for Voltage Output

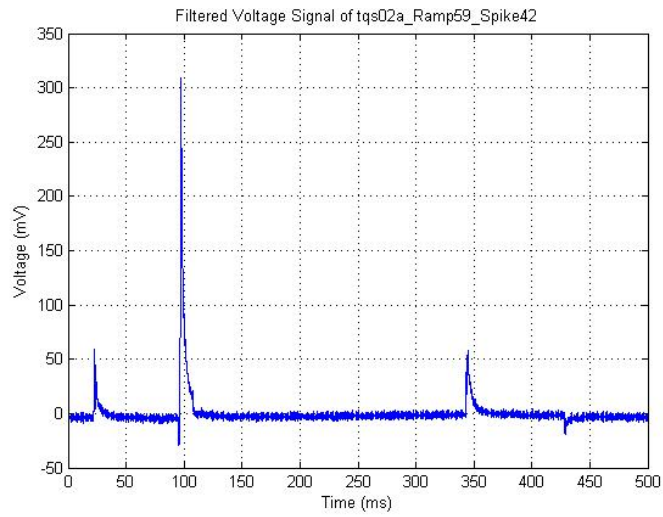


Figure 5: Sample Figure for Filtered Voltage Signal Output

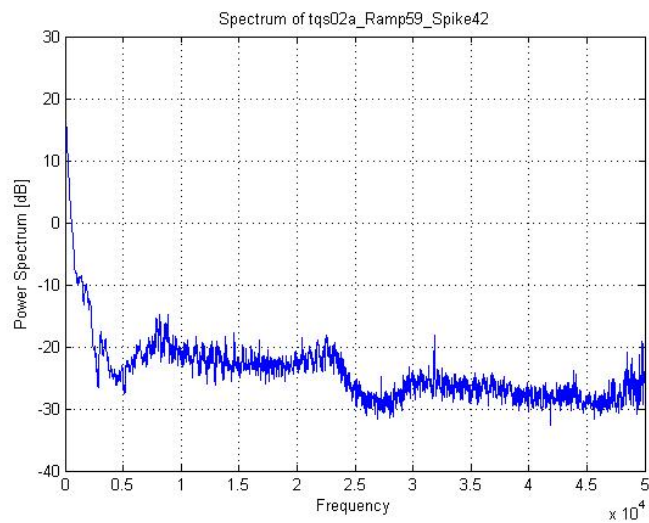


Figure 6: Sample Figure for Spectrum Analyzer Output

▷ Filtered Spectrum Analyzer (Figure 7)

This button has the same functionality as the spectrum analyzer, with the only difference that this button displays the frequency domain of the voltage signal AFTER the filter has been applied.

▷ FFT (Figure 8)

This button displays the Fast Fourier Transform of the voltage signal.

▷ Filtered FFT (Figure 9)

This button displays the Fast Fourier Transform of the voltage signal after the application of the selected (or default) filter.

▷ Numbered Peak Magnitude (Figure 10)

This button displays the filtered voltage signal with the detected spikes marked with a number next to the peak.

▷ View Spikes (Figure 11)

When the user presses this button, the images of the individual spikes within the file processed appear in new windows. From here, the spikes can then be saved if the save option had not been selected.

▷ Save All

By pressing this toggle-button before choosing the file to be processed, the user will save each of the generated images as a JPEG file in the folder from which AVSAP is executed.

▷ Export to Excel (Figure 12)

Pressing this button will open a new window prompting the user for the name of a MS Excel file, title of the worksheet, and cell value of the top-left corner where the data will be exported. The file and worksheet do not need to exist when choosing this option. If this is the case, the program will automatically create them for the user. If the file/worksheet already exists, the program will overwrite this file/worksheet. This property may be convenient whenever the user wishes to export different data into the same worksheet, which can be achieved by writing the exact names of output file and worksheet, and changing the

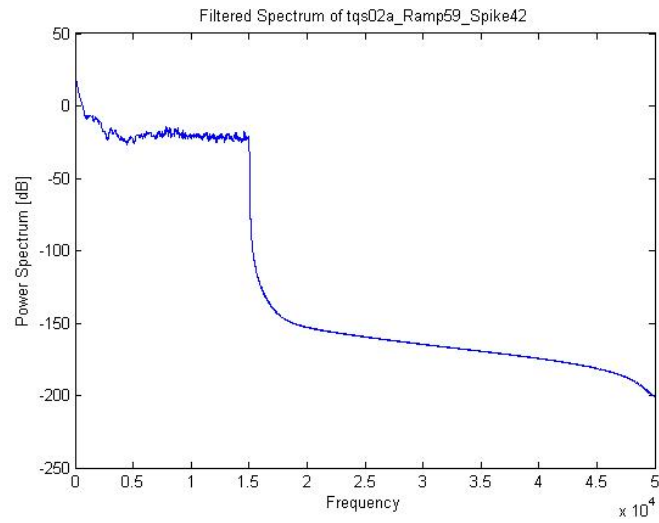


Figure 7: Sample Figure for Filtered Spectrum Analyzer Output

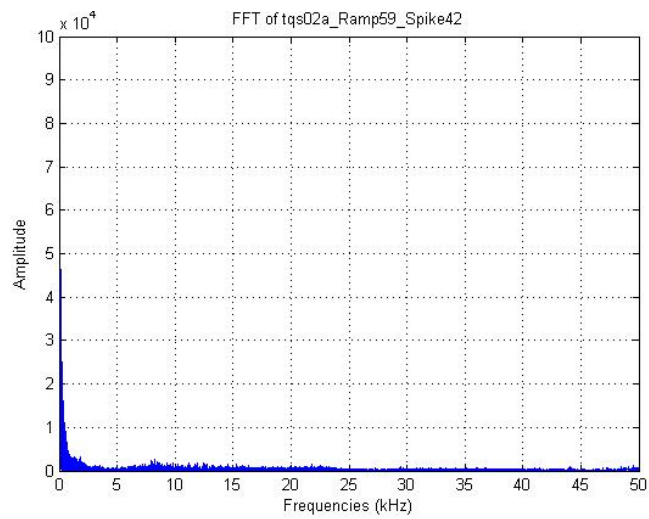


Figure 8: Sample Figure for FFT Output

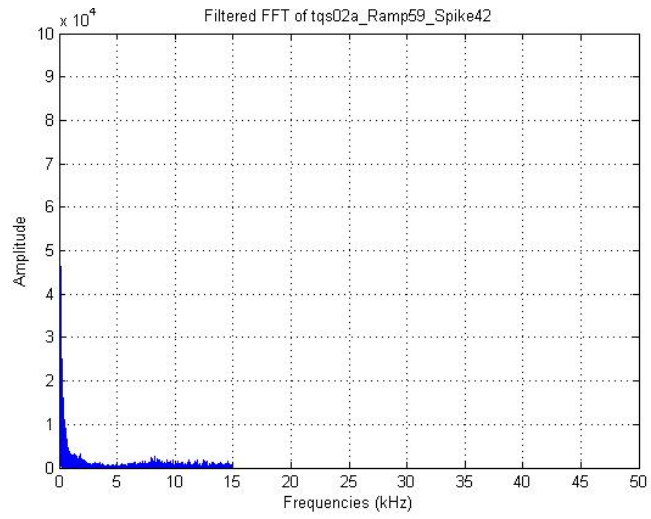


Figure 9: Sample Figure for Filtered FFT Output

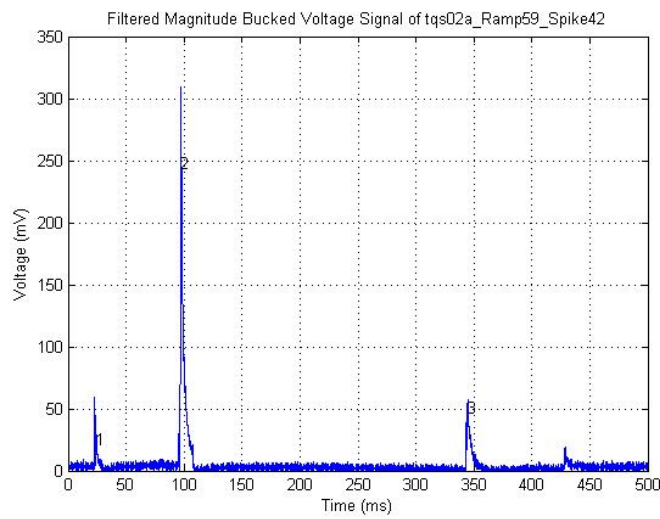


Figure 10: Sample Figure for Numbered Peak Magnitude Output

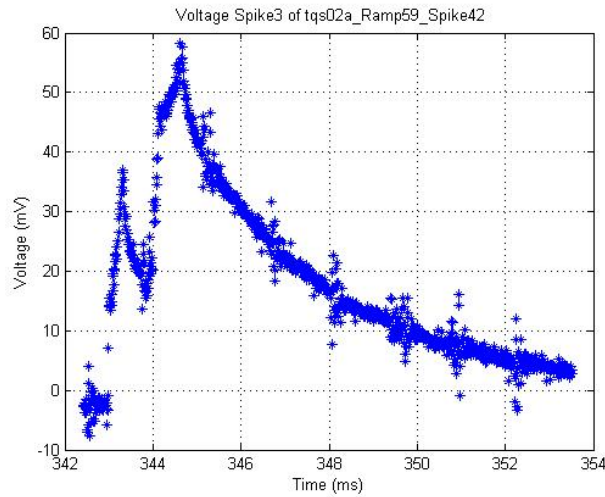


Figure 11: Sample Figure for View Spikes Output

cell value to one that will not cause the new data to overlap with the previously existing data.

3.6. Multiple File Processing Options

If the user selects the many files option from the initial dialog box, a similar GUI to the one in single file processing appears. However, when processing multiple files several of the program’s features are available to the user only if he/she first selects the buttons that correspond to the desired outputs. The program was built in this way due to the potential volume of files that the program is able to generate, which may not be desired by the user

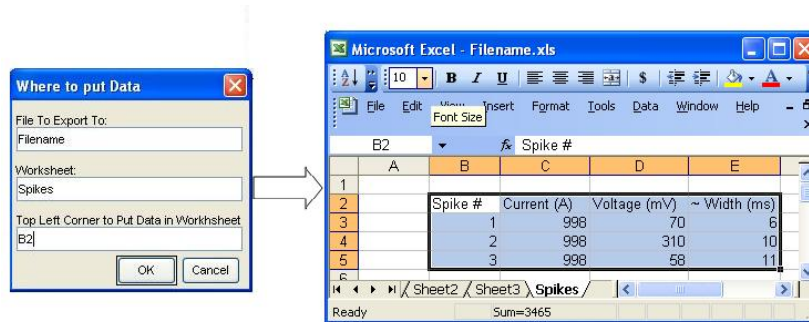


Figure 12: Export to Excel Prompt and Output

at certain instances. The more outputs the user selects, the slower the program will run. Therefore, if the user is looking at a large volume of data but only desires one specific output, he/she can choose that button only and process that data as quickly as possible. All generated JPEG files are given filenames according to the data they represent and will appear in the folder from which AVSAP was executed. Since the Measurement and Analysis Group is mostly interested in a 2D current-voltage (I-V) profile for the spikes detected, this 2D profile is by default the plot appearing after running the program. The functionality of each of the buttons in the multiple file processing platform will be presented next, with graphical illustrations only for those buttons that don't have a counterpart in the single file processing section.

▷ Save Raw Voltage Signals

This option saves one JPEG image of the raw voltage signal versus time for each file that was chosen to be processed by the user.

▷ Save Filtered Voltage Signals

This option saves one JPEG image of the filtered voltage signal versus time for each file that was processed. The amount of noise in this signal will depend on the filter set by the user.

▷ Spike Snapshots

This option saves one JPEG image of every individual spike as detected by AVSAP.

▷ I-V Profile (Figure 13)

This option saves the 2D I-V profile displayed on the axes provided as a JPEG image. The user may choose to either plot absolute values or magnitude and sign of each spike. To understand the meaning of positive and negative voltage values, consider the case of the half coils signal. In such a case, a positive sign in the voltage simply represents coil 1 is at a higher electric potential than coil 2, and vice versa for coil 2. The option of absolute value may be useful whenever the user is not interested in determining which one of the coils was at a higher potential but is rather interested in simply detecting any window of time in which a potential difference was set between the coils.

▷ 3D I-V Profile (Figure 14)

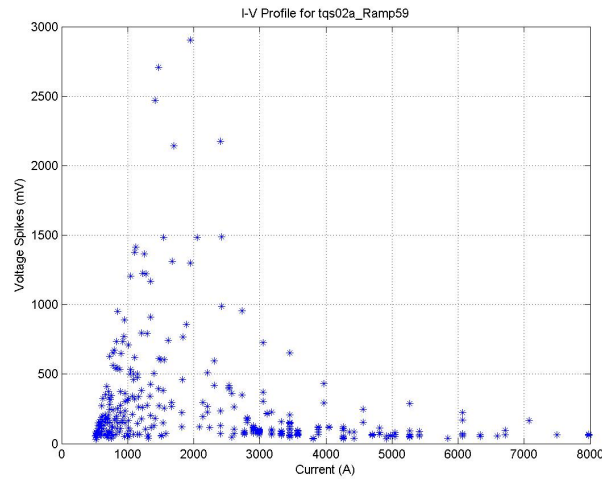


Figure 13: Sample Figure for I-V Profile Output

This option saves a color-coded 3D spike distribution histogram that plots the number of voltage spikes detected as a function of the spike's current and voltage. The two independent variables, which are current and voltage, are plotted on the x and y axes respectively. The dependent variable, which is the number of spikes detected in a specific region, is plotted on the z-axis. This variable has a gradual transition from the smaller wavelengths of the visible spectrum (blue) to larger ones (red) as the number of spikes present in a region increases. This option also creates a new figure window where the user can rotate and translate the histogram in any of the three dimensions in order to focus on the details he/she wishes to show. The user may also save a "static" JPEG image from this window at any time.

▷ Export to Excel

As in the single file processing case, pressing this button will open a prompt that will ask the user for the filename, worksheet name, and cell of the top left corner of the MS Excel file where the data will be exported.

▷ Voltage Histogram (Figure 15)

This option creates a histogram of the total number of spikes detected as a function of the peak voltage of each spike.

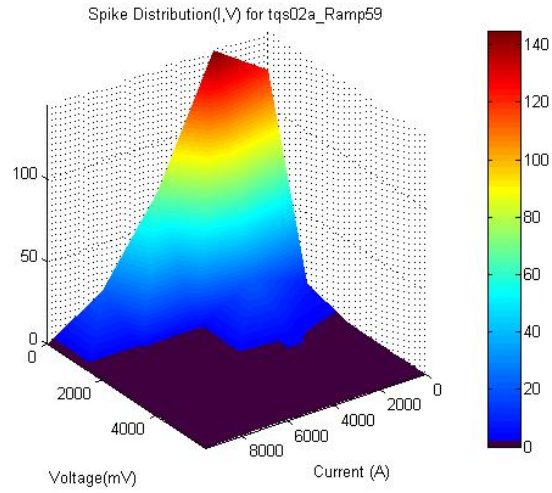


Figure 14: Sample Figure for 3D I-V Profile Output

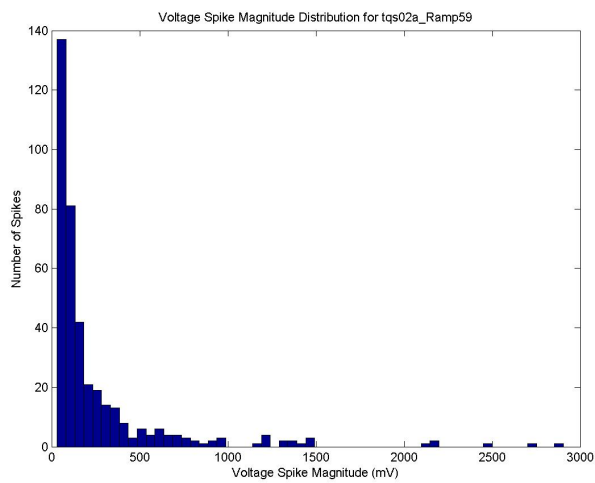


Figure 15: Sample Figure for Voltage Histogram Output

▷ Current Histogram (Figure 16)

This option creates a histogram of the total number of spikes detected as a function of the average current during the half a second of data where the spike was found.

4. Results

Since the early stage of the program's development, the author was told that the success of automating the spike detection process will be measured by how well the spikes detected by the program coincide with the results found by a human inspecting the files. Therefore, to test the results of AVSAP, the spikes detected in Ramp 62 of magnet TQS02a are considered. Conor Donnelly, the author's colleague had inspected this entire ramp searching for voltage spikes prior to the creation of AVSAP. He recorded his finding in a MS Excel spreadsheet containing parallel columns for current and peak voltage at the time of every spike. After the development of AVSAP, in just a few seconds the entire ramp (149 files) was processed and the data was exported to MS Excel in the same format Conor used. Finally, both of these sets of data were graphed on the same axes. The results are shown in Figure 17.

Figure 17 leaves no doubt about the success of AVSAP. Notice how strongly the spikes detected independently by Conor (blue) coincide with those detected by AVSAP (green). There are a few discrepancies however, which are mostly observed at low currents. The reason for this is that once AVSAP filters the signal, the much better SNR allows the program to detect voltage spikes that were previously obscured by noise. Therefore, in general AVSAP detects more spikes in any ramp than the human eye detects. Most of these newly detected spikes are small in amplitude, but there are a few medium sized spikes (100-300 mv) observed in this and other ramps as well. After a detailed inspection of every file in the ramp to understand the nature of this newly detected spikes, the author found out that these were indeed real spikes, and they were commonly "embedded" in larger spikes. Conor had failed to detect these spikes because they were obscured by the high amount of noise present in the data. In conclusion, the expected performance of AVSAP, which was to achieve similar results to the ones obtained by human inspection, was surpassed. After rigorous inspection by the author, Conor, and some members of the Magnet Systems Department, AVSAP was found to be highly efficient in detecting voltage spikes in superconducting magnets.

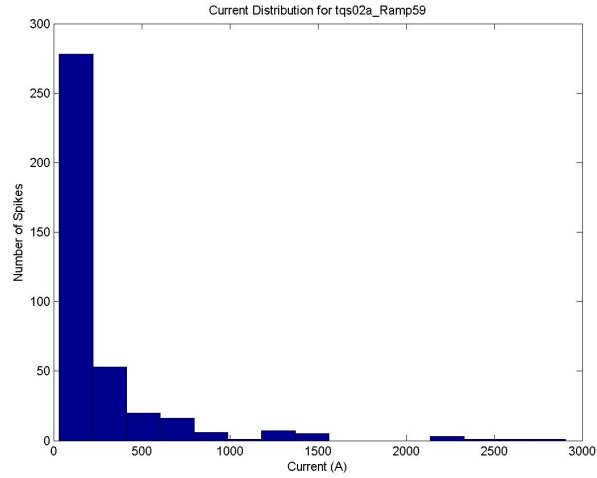


Figure 16: Sample Figure for Current Histogram Output

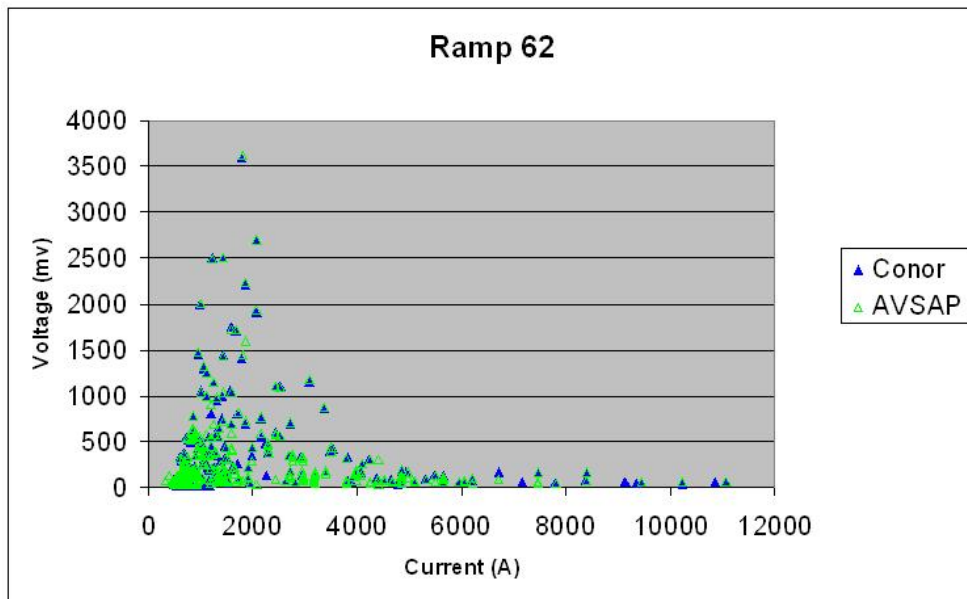


Figure 17: AVSAP v.s. Human Spike Detection

5. A Branch Project: Filtering Analysis for Half Coil Voltage Signals in SC Magnets and Implications for Future Studies

In this section, a typical half coil voltage signal is presented under the effects of different low-pass and band-pass filters. The analysis of different filtering effects on the signal started as a secondary "branch" project while creating AVSAP, in an effort to improve the performance of the spike detection algorithm by reducing the amount of noise obscuring the signal. This branch project may have great implications for future voltage spike studies at Fermilab, since the detection of small spikes and the structure of all spikes have been obscured by the high amount of noise present in the signal of interest.

It is important to note that the filtering here presented is applied to the already captured signal by the VSDS, meaning this is a software effect rather than a hardware effect. However, once a certain filtering technique proves (via software modeling) to lower the noise level at an acceptable signal reduction cost, a suitable physical filter (hardware) may be applied at the source. To determine the characteristics of the most suitable filter for this application, the signals under consideration and their spectral components need to be well understood. Ultimately, applying an adequate filter will increase the SNR (signal to noise ratio), which will lead the magnet systems department into detecting voltage spikes that are smaller in amplitude than the present spikes being detected. This is based on the functionality of the VSDS, whose data capturing system if not triggered by spikes at a level lower than the present noise level. Furthermore, a physical filter at the source will also provide insight into the true structure of the voltage spikes of interest. Therefore, the importance of increasing the SNR cannot be underestimated.

5.1. Previous Filtering Analysis

In the interest of studying flux jumps in superconducting accelerator magnets, several attempts have been made at Fermilab to improve the SNR of the voltage spike train representing these flux jumps. In his Ph.D. Thesis, *Thermo-magnetic Instabilities in Nb₃Sn Superconducting Accelerator Magnets* [11], Bordini proposed two different band-pass filters (the second replacing the first) to be adopted by the VSDS in order to improve the SNR. The results obtained for a typical voltage signal after being exposed to both of these filters are here presented. As a reference, the following analysis was done for file "tqs02a_Ramp59_Spike26.mat". The current and voltage signals are shown in Figures 18

and 19 respectively, followed by the spectral components (FFT) of the voltage signal in Figure 20.

1.- *First Filter*

The first filter proposed by Bordini was a band pass filter that rejects frequencies below 1500 Hz and above 30 kHz. The portion of the spectrum that is accepted after applying the filter may be seen graphically in Figure 21 by switching to the frequency domain by means of the FFT. Although Figure 21 may seem to not coincide with the same part of the spectrum shown in Figure 20, note that the scale on the y-axis has changed. This scale was changed by the suppression of the high amount of low-frequency components present in the signal prior to the filtering. The result of reconstructing the signal with the allowed frequencies by means of the IFFT is shown in Figure 22.

2.- *Second Filter*

The second band-pass filter proposed by Bordini holds the upper bound of the filter at 30 kHz, but takes the lower bound to 800 Hz. The signal under consideration is shown in the frequency domain (FFT) after applying this second filter in Figure 23. Figure 24 shows the reconstructed signal by means of the IFFT after the application of this filter.

A glance at both reconstructed signals leaves no doubts about the catastrophic results obtained by applying any one of the filters suggested by Bordini in [11]. The structure of the spikes has been completely lost. Furthermore, by comparing any of these images to the original signal, it is evident that there is very little improvement in the SNR. In light of these results, the author was led to look for different filtering approaches.

5.2. A Series of Low-Pass Filters

By inspection of the original voltage signal, Figure 19, it appears that the frequencies of the noise are of greater magnitude than those of the spikes. The high amount of low frequency components present in the signal can be seen in its FFT, Figure 20. This latter fact hints that suppressing the lower end of the spectrum may lead to catastrophic results. Therefore, it is reasonable under these two premises to apply a low-pass filter rather than a band-pass filter to increase the SNR.

To fully understand the effect of any filter on a signal, two things (at least) need to be considered:

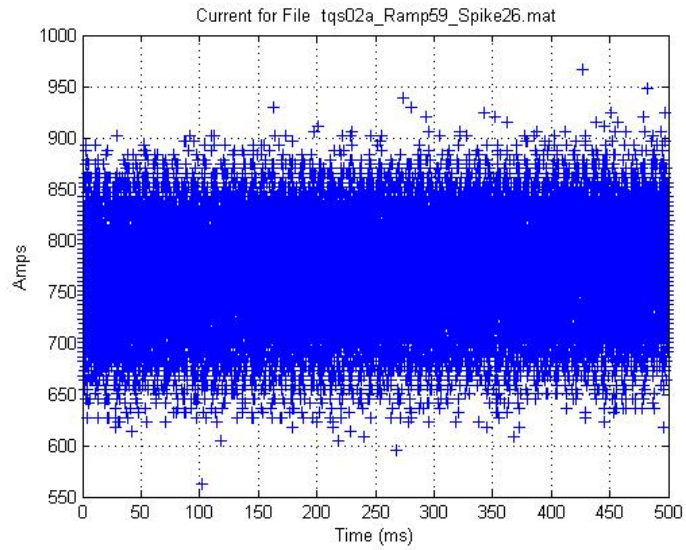


Figure 18: Current signal for the file under consideration

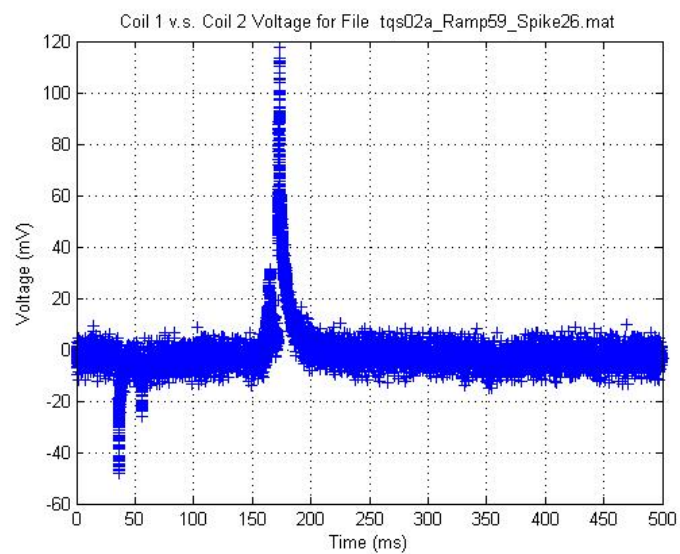


Figure 19: Voltage Signal Prior to Filtering.

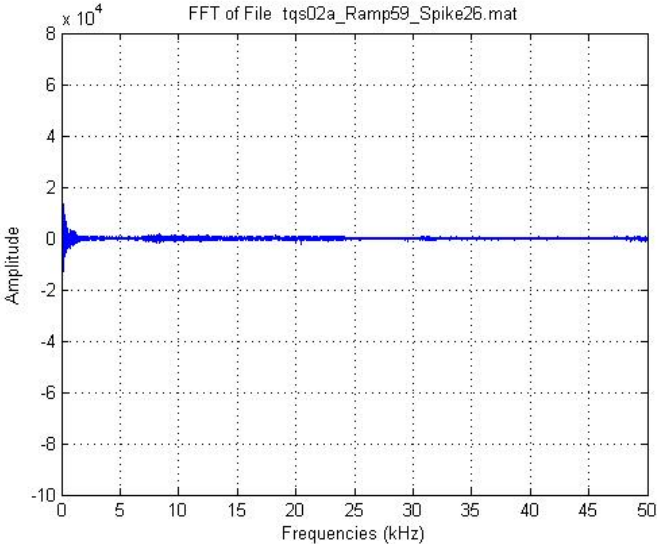


Figure 20: Spectral Components of the Voltage Signal to Which the Filter is Applied.

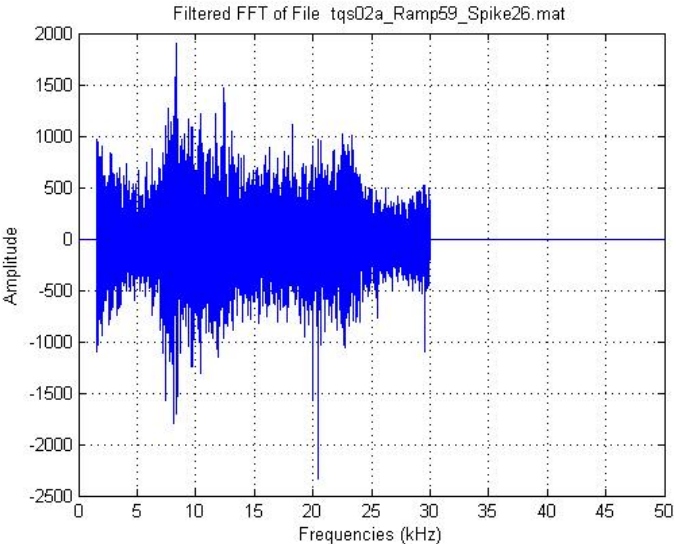


Figure 21: Accepted Spectral Components of Voltage Signal After First Filter

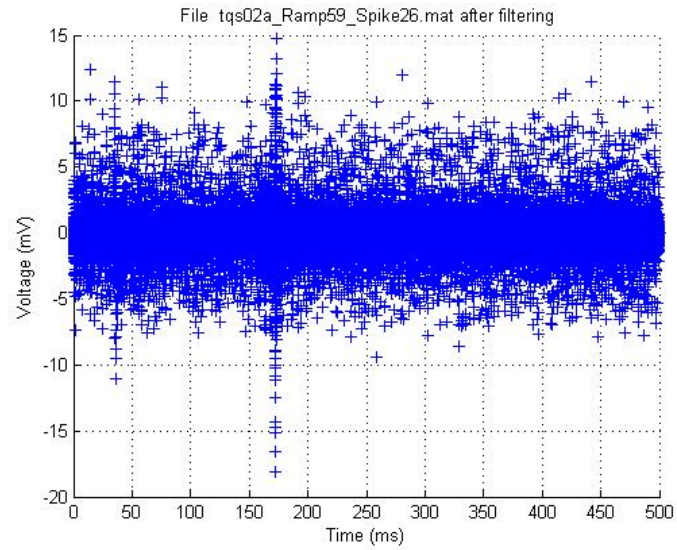


Figure 22: Reconstructed Voltage Signal After First Filter

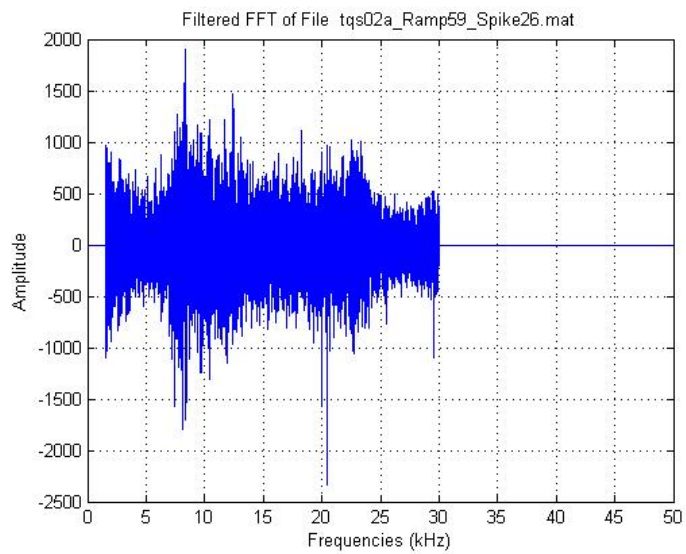


Figure 23: Accepted Spectral Components of Voltage Signal After Second Filter

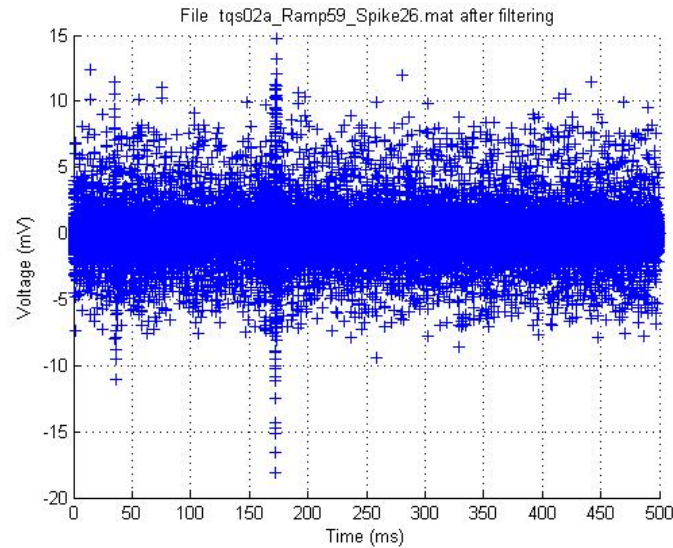


Figure 24: Reconstructed Voltage Signal After Second Filter

1. How is the noise affected by the filter ?
2. How is the signal of interest affected by the filter ?

To study both of these effects, the same voltage signal presented in section 5.1 is considered. The results from the application of a series of low-pass filters with an upper limit at 30, 25, 20, and 15 kHz are shown in Figure 25.

In communication theory, SNR at time t is defined as the amplitude of the signal at time t divided by the standard deviation of the noise. However, based on the DAQ triggering system used by the VSDS, which relies on a simple amplitude threshold approach, this definition of SNR may not be best suited to determine what the most suitable filter is for this specific application. Since any data point greater than the threshold will trigger the DAQ system, no threshold below the highest data point arising from noise should be set, regardless of the standard deviation of the noise. Therefore, it is more reasonable to study the effect of the filter on the "envelope" of the noise for a certain period of time rather than on its standard deviation. This "noise envelope" for the signal under consideration is shown in Table 1, where E^- and E^+ are the lowest and highest values of the envelope, and (ΔE) is the total envelope size. The data considered to be part of the envelope was that obtained during the first 30 ms of time, where there was no spike present.

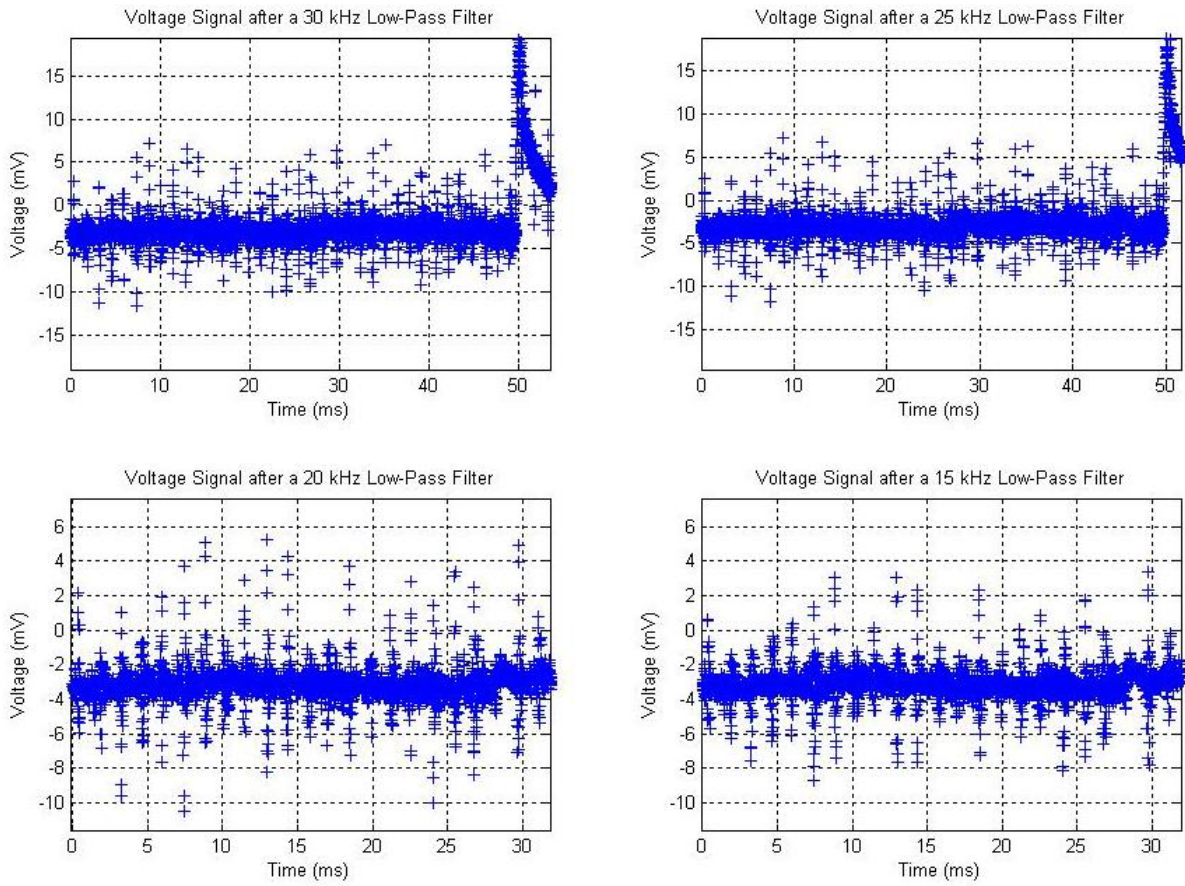


Figure 25: Effects of Different Low-Pass Filters on Noise

Filter / Envelope	E^- (mV)	E^+ (mV)	ΔE (mV)
No Filter	8	-12	20
30 kHz	8	-12	20
25 kHz	8	-12	20
20 kHz	5	-10.5	15.5
15 kHz	3.5	-8.5	12

Regarding the second issue, which is on how the signal of interest is affected by the filter, a new algorithm was integrated with AVSAP in order to determine these effects. Once AVSAP detected the voltage spikes after the application of the previously mentioned filters, the new algorithm obtained a newly defined parameter called SRR (Spike Reduction Ratio). The SRR is obtained by comparing the magnitudes of the peak voltages of the spikes after, V_2 , and before, V_1 , the filtering. The SRR provides the percent reduction in amplitude of a spike after the application of a filter.

$$SRR = 1 - \frac{V_2}{V_1} \quad (3)$$

From 3, its clear that a SRR of 0 means that a spike had no reduction at all, while a SRR close to 1 means the spike was affected drastically. To visualize how all the spikes in a ramp were affected, as well as how much they were affected, normalized distributions of SRRs for all spikes within a ramp were generated for all four filters (Figures 26 - 29). From these distributions, the reader may see that in any of the filters here presented, the vast majority of the spikes (90 % +) suffered a reduction in their amplitude of less than 5 % (SRR < 0.05). The greater reduction of the spikes as the band of allowed frequencies is shortened is clear.

5.3. Choosing an Adequate Filter

From Table 1 in section 5.2, it is evident that a 30 kHz and even a 25 kHz provide no improvement in noise reduction. 20 and 15 kHz filters on the other hand, provide a 25 and 40 percent improvement on the reduction of the noise envelope. However, from Figures 28 and 29 it may be seen that some of the spikes in the ramp start having a great reduction in their amplitudes as well, which is highly undesirable. Therefore, one last analysis was done to determine what kind of spikes are being affected the most by the filtering. For

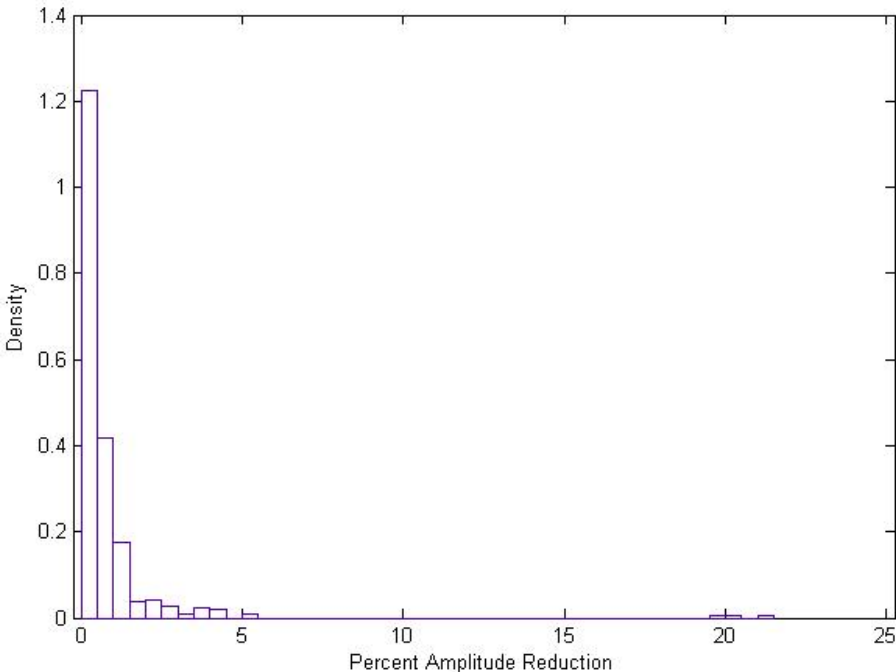


Figure 26: SRR Distribution After a 30 kHz Low-Pass Filter

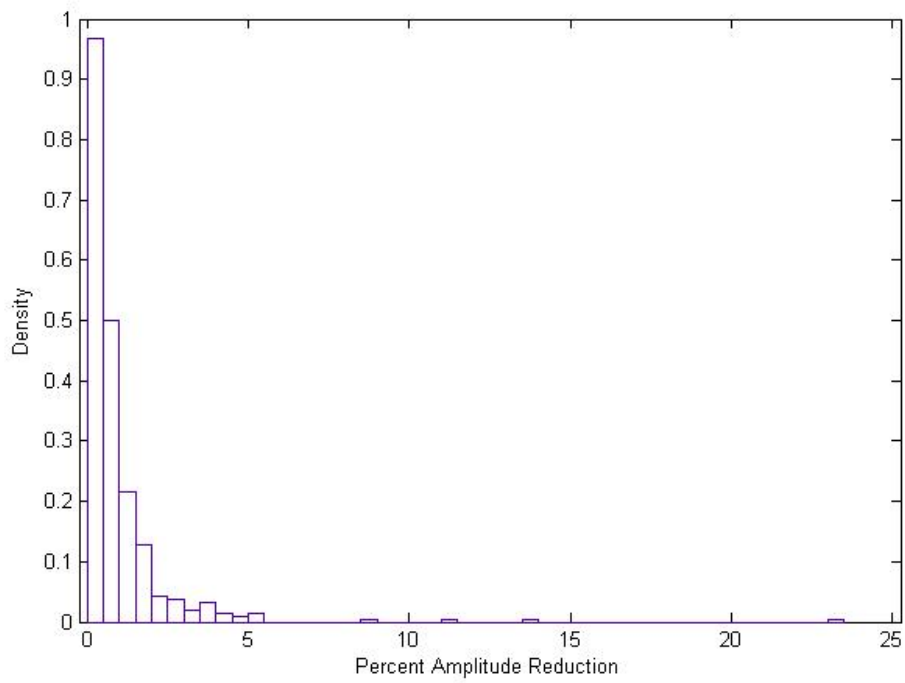


Figure 27: SRR Distribution After a 25 kHz Low-Pass Filter

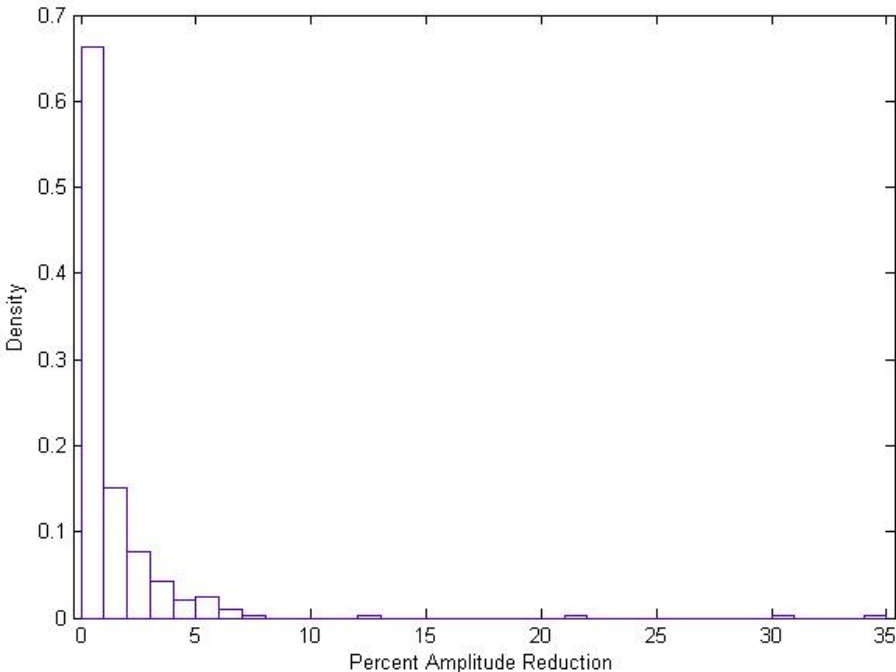


Figure 28: SRR Distribution After a 20 kHz Low-Pass Filter

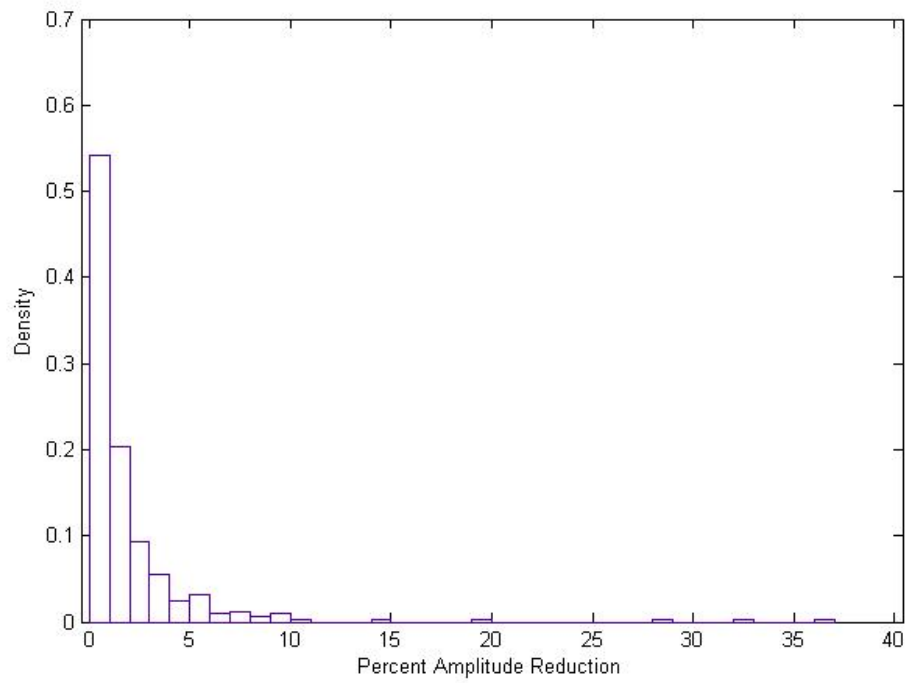


Figure 29: SRR Distribution After a 15 kHz Low-Pass Filter

this purpose, the new algorithm was modified to find those spikes that were reduced by more than 10 % in their amplitudes ($SRR > 0.1$). Normalized distributions of these results are shown in Figures 30-33. What is normalized in these figures is the area inside the rectangles, which represents the fraction of spikes that having $SRR > 0.1$. The small amplitudes of all these spikes is clear.

By looking at the actual numbers generating the statistics shown in Figures 30-33, the following facts stand out:

1. The greatest amplitude for any spike with a $SRR > 0.1$ was 83.3 mV. (observed in the 15 kHz filter)
2. The average amplitude of all spikes with a $SRR > 0.1$ in all the filters was 19.42 mV.
3. Spikes with $SRRs > 0.15$ were in their vast majority less than 20 mV.

It is important to note that the voltage threshold set at the VSDS by the scientist ramping this magnet in this case was 50 mV. For all spikes with an $SRR > 0.1$ which are shown in Figures 30-33, only 2 of these spikes were above 50 mV in amplitude prior to the filtering. The original amplitudes of these two spikes was 70.5 and 83.3 mV, and they were reduced to 60.5 and 74.9 mV respectively. The total number of spikes found for this ramp was 425. These facts imply several things, which are listed below.

1. In the cases where the $SRR > 0.1$, the spikes were found to be very small in amplitude (below the VSDS threshold) for all filtering above 20 kHz. This means these spikes would have not even been captured by the VSDS. After taking a closer look at the data, the author realized these spikes were found solely because they were embedded in greater spikes which were the ones that actually triggered the capturing of the event.
2. The two spikes with a $SRR > 0.1$ in the 15 kHz filter, were only affected by 14.1 % and 10.1 % respectively, which is not catastrophic for the focus of this research. By looking at the big picture of the spikes detected in a typical ramp (Figure 17), the reader may see what a small contribution these spikes may have in the general current-voltage profile the Magnet Systems Department is looking for in order to characterize these spikes.

In conclusion, this study revealed it is absolutely safe to apply a 20 kHz low-pass filter at the source while maintaining the SRR below 0.10 for all spikes. Furthermore, it is evident from Figure 28 that the application of this filter will result in a SRR of less than 0.04 for

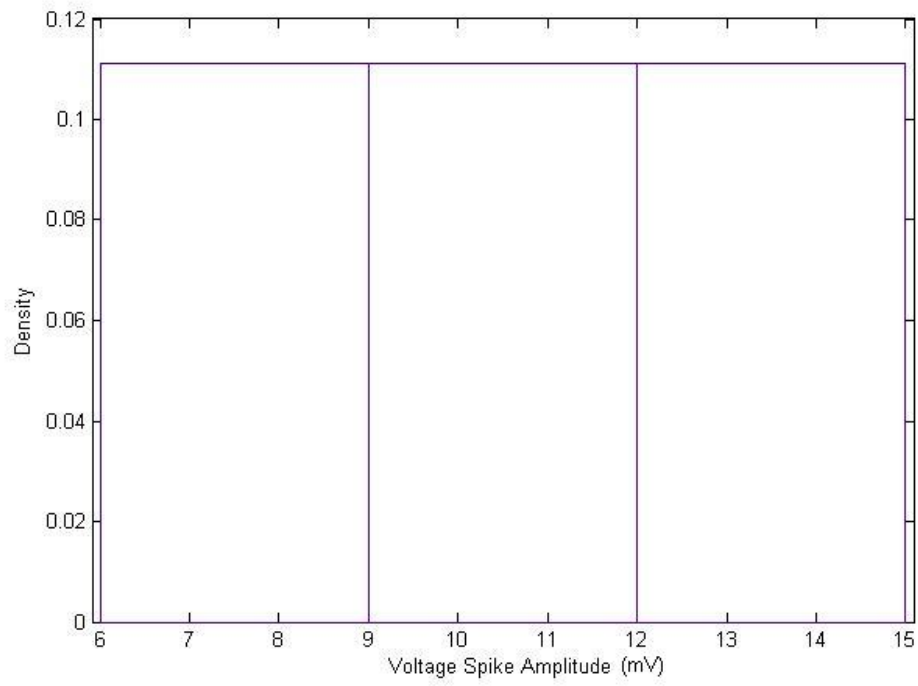


Figure 30: Distribution of Spikes with SRRs Above 0.1 After a 30 kHz Low-Pass Filter

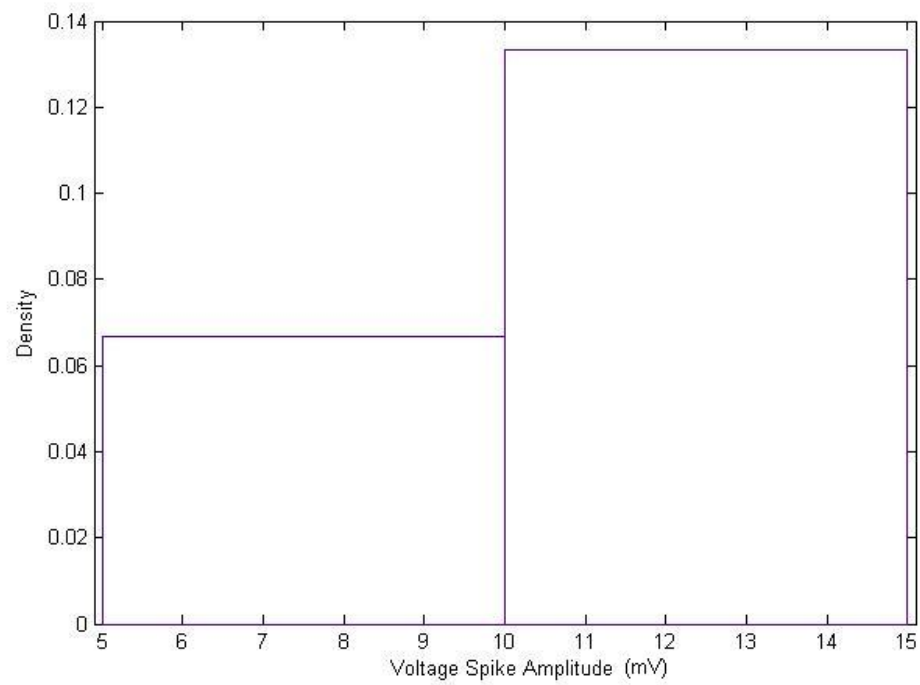


Figure 31: Distribution of Spikes with SRRs Above 0.1 After a 25 kHz Low-Pass Filter

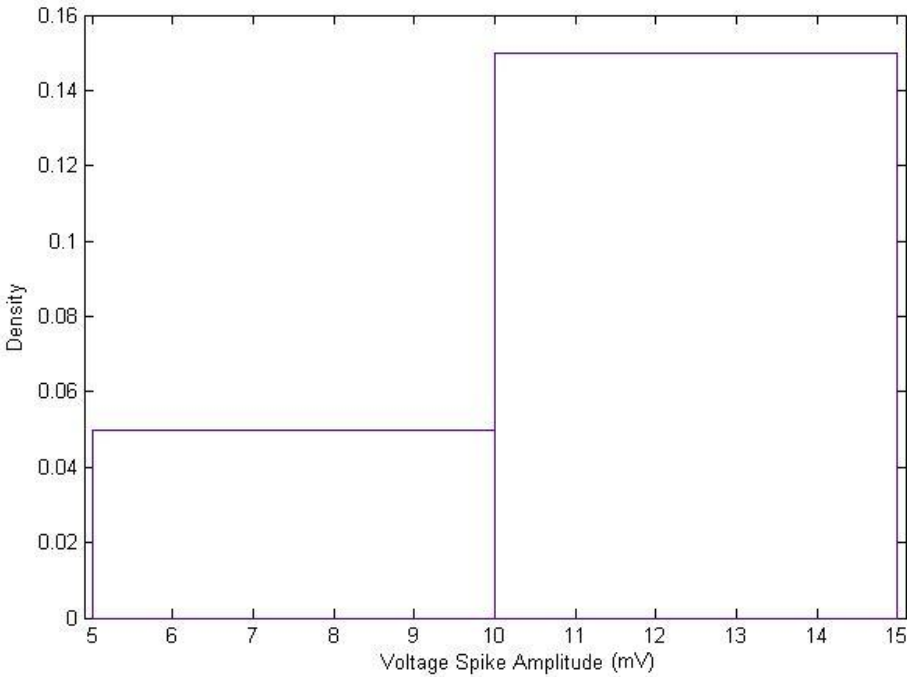


Figure 32: Distribution of Spikes with SRRs Above 0.1 After a 20 kHz Low-Pass Filter

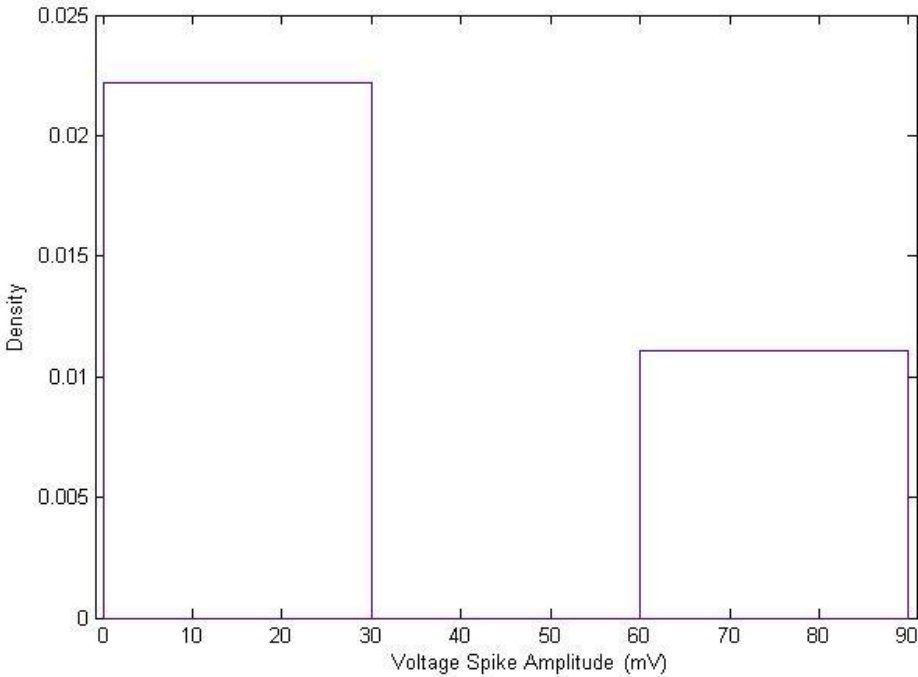


Figure 33: Distribution of Spikes with SRRs Above 0.1 After a 15 kHz Low-Pass Filter

over 90 % of the spikes, and less than 0.01 for nearly 65% of the spikes. The gain here in noise reduction is roughly 25 %.

With the application of a 15 kHz filter, noise is reduced by 40 %. However, 2 spikes (out of 425) were affected by 14.1 % and 10.1 %. The author still believes the application of the 15 kHz low-pass filter is more convenient, since the SNR is improved much more and the cost in spike reduction seems acceptable. Ultimately, the decision on the characteristics of the applied filter (if any) will rely on the Magnet Systems Department.

6. Conclusions

A software capable of autonomously detecting voltage spikes in superconducting magnets, cables, and strands has been developed. The results were found to be better than the expected, by surpassing the expectations of simply detecting the same spikes detected by the human eye. After the author's departure from Fermilab, AVSAP will remain at Fermilab for future studies of these thermo-magnetic instabilities in superconductors. Also, a detailed study on the effect of different filters on the voltage signals containing the spikes of interest was done. Statistics were generated, and conclusions were drawn that may serve as a reference for the future application of a filter at the source in order to improve the SNR and thus the spike detection system.

7. Acknowledgments

First and foremost, I state my deepest appreciation to my parents, Abbas and Genoveva, for their love and support.

I am also deeply grateful to my supervisor, Michael Tartaglia, who has been an excellent guide in this wonderful learning experience at Fermilab.

I also state my gratitude for all the individuals and organizations that make it possible for students to gain an invaluable experience in scientific research such as the one I obtained at Fermilab. Thanks to the Department of Energy for funding these activities, to Fermilab, to the entire Magnets Systems Department, and special thanks to the Measurement and Analysis Group for the valuable input provided while developing my work here.

Many thanks to Conor Donnelly, who provided valuable input while developing the program and created AVSAP's graphical user interface.

Last, but certainly not least, thanks to my university (ERAU) for the high-quality education I have received from the great faculty there present. Special thanks to the faculty members from the Physical Sciences Department and the College of Engineering who have "walked the extra mile" with me in my slow but joyful learning process.

References

- [1] V. V. Schmidt, *The Physics of Superconductors*, Nauka Publishers, Moskau 1982.
- [2] M. N. Wilson, *Superconducting Magnets*, Clarendon Press, Oxford 1983.
- [3] K.-H Mess, P. Schmüser, S. Wolff, *Superconducting Accelerator Magnets*, World Scientific Publishing Co., Singapore 1996.
- [4] R. G. Mints, "Flux creep and flux jumping", *Physical Review B*, vol. 53 no. 18, pp. 12311-12317, May 1996.
- [5] D. F. Orris et al., "Voltage Spike Detection in High Field Superconducting Accelerator Magnets", *IEEE Trans. Appl. Superconductivity.*, vol 15, no.2 , June 2005.
- [6] B. Bordini et al., "Voltage Spike Studies of Nb₃Sn and NbTi Strands", *IEEE Trans. on Applied Superconductivity*, vol. 15, no. 2, June 2006
- [7] V.V. Kashikhin and A.V. Zlobin, "Magnetic Instabilities in Nb₃Sn Strands and Cables", *IEEE Trans. on Applied Superconductivity*, vol. 15, no. 2, June 2005.
- [8] G. Ambrosio et al., "Measurement of Critical Current and Instability Threshold of Rutherford-type Nb₃Sn Cables", presented at *19th International Conference on Magnet Technology*, Genova, Italy, September 18-23, 2005 conference.
- [9] S. Feher et al., "Sudden Flux Change Studies in High Field Superconducting Accelerator Magnets", *IEEE Trans. Appl. Superconductivity.*, vol 15, no.2 , June 2005.
- [10] E. Barzi et al., "Instabilities in Transport Current Measurements of Nb₃Sn Strands", *IEEE Trans. Appl. Superconductivity.*, vol 15, no.2 , June 2005.
- [11] Bernardo Bordini, "Thermo-magnetic Instabilities in Nb₃Sn Superconducting Accelerator Magnets" (Ph.D. dissertation, Pisa University, 2007).

A. AVSAP GUI

The following image was captured by a "Print Screen" when running AVSAP in single file processing. The multiple file processing GUI looks the same; only the buttons' functionalities vary as described in section 3.6.

